

Research Article

Observation of Glass Nanophase Separation from TEM Fresnel Contrast Images

Shangcong Cheng

National Center for Electron Microscopy, Lawrence Berkeley National Laboratory, Berkeley, CA 94720, USA
E-mail: shangcongcheng@lbl.gov

Received: 19 August 2022; **Revised:** 18 October 2022; **Accepted:** 21 October 2022

Abstract: Properties of phase-separated glasses, such as mechanical strength, chemical durability, and optical transmission, change drastically with the sizes and types of phase separation. Characterizing glass phase separated structures at the nanometer scale is vital for establishing the structure-property relation of various glass systems. This work will first briefly review the “staining” technique previously used to reveal the nanodroplet phase separation in Pyrex glass and its limitations. It will then introduce the TEM Fresnel contrast technique for studying glass structures. The theoretical background, practical application procedures, and examples of the method are described.

Keywords: nanophase separation; borosilicate glass; soda-lime-silica glass; TEM Fresnel contrast image; energy dispersive X-ray spectroscopy; electron energy loss spectroscopy

1. Introduction

In order to establish the structure-property relation of various glass systems, it is necessary to characterize glass phase separated structures at the nanometer scale. Transmission electron microscopy (TEM) techniques have been used to study the structures of glass phase separation for many years. A large number of phase separation TEM images of glasses with various compositions and thermal histories have been presented in many papers as well as several books [1–5]. However, in these studies most TEM results were obtained from specimens prepared by using the carbon replica technique or from glass fragments without large thin areas. Thus, in these investigations the space resolution was limited to about 10 nm and the analytical capabilities of TEM were not fully utilized. In order to investigate the origin of phase separation in glasses and to correlate the properties of phase separated glasses with their nanostructures, the resolution of TEM observation needs to be better than 10 nm. The purpose of this work is to describe two TEM methods: the “staining” technique and the Fresnel contrast technique. Both have spatial resolution higher than the traditional carbon replica technique and are capable of revealing glass phase separation on the nanometer scale (<10 nm). The “staining” technique and its limitations will be briefly reviewed. The emphasis is to describe the TEM Fresnel contrast technique and to illustrate the convenience and reliability of the technique using published experimental results.

2. Observation of nanophase separation in glasses by staining technique

In 1969, R. H. Doremus and A. M. Turkalo of GE reported for the first time their staining method for revealing the nanophase separated structure in commercial borosilicate Pyrex glass [6,7]. Pyrex glass is an important technical glass invented by Corning Inc. during the 1910s [8]. Pyrex glass shows great chemical durability and thermal shot resistivity and is widely used for laboratory ware and kitchenware. Because the phase separated structure in the normal Pyrex glass is on a scale of less than 10 nm, it had never been directly observed in TEM before 1969. In Doremus and Turkalo's work, the fine phase separation in Pyrex glass was made visible in TEM by exchanging heavy element silver ions with light element sodium ions in the glass [6,7]. The image contrast of the staining technique arises due to the difference in the elastic scattering power of the two phases of the specimen. When the light element in one phase was replaced by a heavier element, the elastic scattering power of the light element rich phase significantly increased. Thus, more electrons scattered from the light element rich phase are blocked by the objective lens aperture and the contrast between the two phases was enhanced. Without the ion exchange, the diffraction contrast of the glass specimen at the objective lens focus condition would have been too low to be observed. The Doremus and Turkalo's TEM photograph taken from Pyrex glass, in which silver ions have been changed for sodium ions, shows about 3 nm in size of the droplet structure. Prior to use the staining technique, TEM specimens for imaging the phase structure in Pyrex were prepared by the carbon replica technique, and the fine structures on the scale of about 3 nm could not be observed. Only separated phase structures could be observed, where the sizes of phases grew to larger than 10 nm after heat treatments of the specimen.

Although Doremus and Turkalo successfully revealed the nanophase structure in the borosilicate Pyrex glass, they did not find any evidence of phase separation in the commercial soda-lime-silica glass after applying the same staining method. The photograph taken from the edge of a large splinter of soda-lime-silica glass with staining by silver does not show phase separated structure in the specimen. This result contradicts with experimental evidence by X-ray absorption spectroscopy and neutron diffraction, which indicate the existence of silica rich and alkali/alkaline earth rich regions in the structure of soda-lime-silica glass [9–11]. The commercial soda-lime-silica glass is now known to have the spinodal type of phase separation [12,13]. Therefore, the application of the staining technique used by Doremus and Turkalo is limited; it may work well to reveal the droplet type of phase separation but not the spinodal type. This may be explained as the following: the droplet type of phase separation has clear and sharp boundaries between the two separated phases; while the boundaries in spinodal phase separation are defused and interconnected. For practical investigation of the phase structure of glasses, it would be desirable to use a more convenient and reliable method.

3. Observation of nanophase separations in glasses by TEM Fresnel contrast imaging

In 2015 Cheng et al. reported for the first time, the application of TEM Fresnel contrast imaging technique to examine nanophase structures of various commercial Pyrex glass cookware [12]. Then in 2017 TEM Fresnel contrast was applied again to correlate the indentation cracking behavior with the structures of nanophase separation of glasses [13]. These results show that the Fresnel contrast technique is well suited to characterize nanophase structures of glasses. This work explains in more detail the technical background of TEM Fresnel contrast images, and how it was used to study the nanophase separation of glasses in more detail, with the purpose of encouraging its further applications in the field of glass related research.

Fresnel contrast images are a kind of phase contrast images and obtained with the objective lens several microns out of focus. The image contrast is not dependent on the scattering power but on the inner potential of specimens [14]. In TEM experiments, Fresnel contrast images are often observed at the edge of the specimen or a small hole in the specimen. Figure 1 are images of a hole in an amorphous carbon film illuminated with a parallel electron beam. Figure 1(a), 1(b) and 1(c) show that when the objective lens is in the conditions of underfocus, overfocus and exact focus, fringes round the edge of the hole are bright, dark and nonvisual, respectively [14]. The size of the hole in Figure 1 is about 50 nm. The Fresnel contrast method is a routine technique for correcting astigmatism of objective lens in TEM operation. If the hole size in Figure 1 is only a few nm, the bright or dark circles around the hole would be bright or dark spots, respectively. The bright and dark spots of Fresnel contrast images are indications of existing nanosized areas with a different inner potential

from the adjacent region in the specimen. This method was successfully used to reveal gas bubbles with nanometer scale inside nuclear materials in the 1970s [15]. Figure 2(a) and 2(b) are images of nanosized He bubbles in Au matrix in overfocus and underfocus conditions [14,15]. The contrasts illustrated in Figure 2 demonstrate that Fresnel contrast technique could reveal nano sized regions which have different inner potential from the surrounding area. More details of the calculation about Fresnel contrast and its applications can be found in the references [14–16]. This work focuses on the new application of TEM Fresnel contrast technique in glasses, where it is used to study nanophase separations in borosilicate Pyrex glass and soda-lime-silica glass.

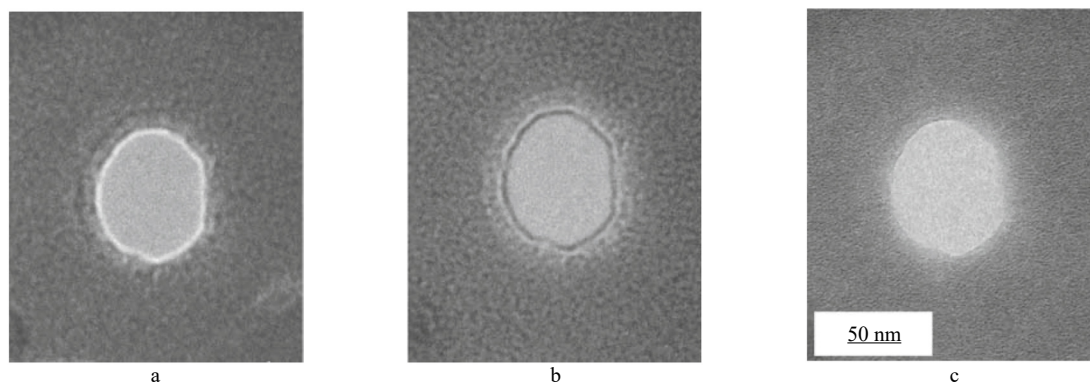


Figure 1. Images of a hole in an amorphous carbon film illuminated with a parallel electron beam. Figure 1(a), 1(b) and 1(c) show that when the objective lens is in conditions at underfocus, overfocus and exact focus, fringes round the edge of the hole are bright, dark and nonvisual, respectively. Reproduced from Ref. [14].

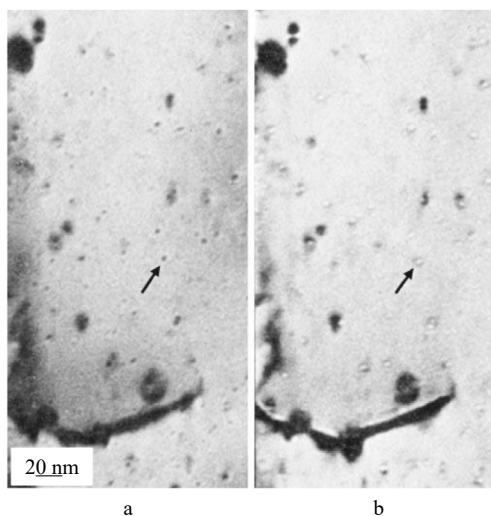


Figure 2. Images of nanosized He bubbles in Au matrix in (a) overfocus and (b) underfocus conditions. Reproduced from Ref. [14].

3.1 Experimental procedures

Borosilicate Pyrex glass and soda lime silica glass were chosen for the experiments. Since the samples are similar to those used by Doremus and Turkalo [6], the results can be compared with the previous works.

The nanophase structures of glass specimens were examined using a CM300 TEM and CM200 TEM (Philips, Amsterdam, The Netherlands), which is attached with an Oxford INCA Energy Dispersive X-ray Spectroscopy (EDS) detector and a Gatan Imaging Filter, having 1 nm space resolution and 0.9 eV energy resolution. In this study EDS

and Electron Energy Loss Spectroscopy (EELS) were used to monitor possible chemical and structural changes in the specimens caused by the electron beam during TEM imaging.

The glass samples were mechanically polished to a thickness of about 10 nm by dimpling. The final thinning of the sample to electron transparency was carried out using a Gatan PIPS ion mill. The acceleration voltage of the ion beam was 6 kV with final thinning at 3 kV at a 7° incident angle. The specimens were coated with a thin carbon layer in a vacuum chamber before TEM observation to minimize charging during TEM imaging

3.2 Results for borosilicate Pyrex glass

It was found that the Pyrex glass specimen is stable under normal TEM observation conditions. The use of Fresnel contrast images to study the droplet nanophase structure of Pyrex glass is straightforward. Figure 3(a–c) are Fresnel contrast images of the specimen without staining, taken near focus, underfocus at about 2 μm and overfocus at about 2 μm, respectively. As expected, the image of Figure 3(a), taken in focused condition, does not show any visible contrast of phase separation. However, the images in Figure 3(b) and 3(c), taken out of focus, clearly show a droplet phase almost uniformly dispersed in the matrix. The results of Figure 3 indicate that average inner potentials of the B rich phase and the Si rich phase in borosilicate Pyrex are different. The incident electron beam is a plane wave, and different regions of the glass specimen impart different amounts of phase change to the exit wave. At the Fresnel defocus condition, the electron beams, having passed through different regions, interfere together to produce the Fresnel contrast. It should be noted that the contrast in Figure 3(b) and 3(c) images is reversed because of the reversed defocusing conditions. The droplet phase in Figure 3(b) and 3(c) is estimated to be around 3 nm in diameter and agrees with that obtained early by the staining technique.

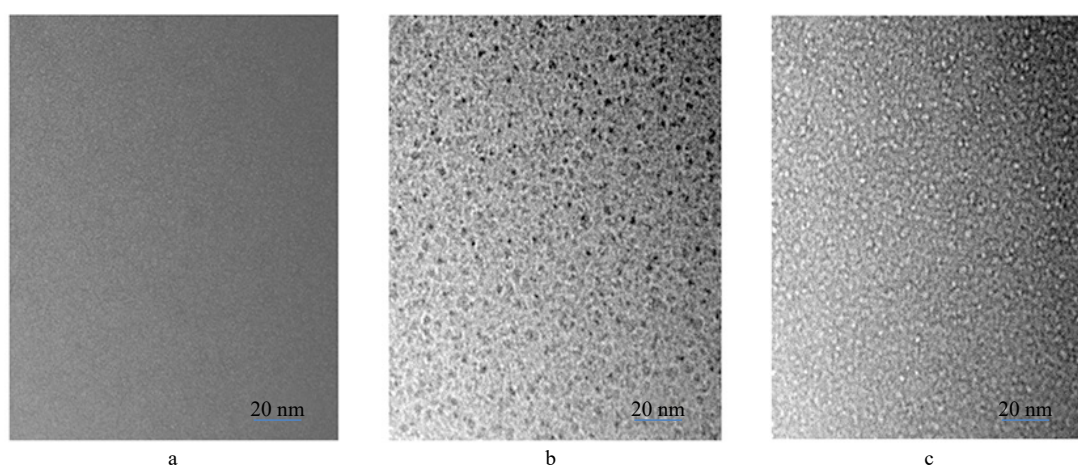


Figure 3. Fresnel contrast images of the specimen without staining, taken near focus (a), underfocus about 2 μm (b) and overfocus about 2 μm (c), respectively.

3.3 Results for soda-lime-silica glass

The use of Fresnel contrast images to study the nanophase structure of soda-lime-silica glass is more complicated due to the electron beam irradiation effects. It is well known that when exposed to irradiation by laser or by electron beam, the Na and Ca ions in soda-lime-silica glasses are easily separated from the glass network and migrate out from the exposed area. The number of migrated ions is dependent on the radiation dose [17–19]. This is because the single bond strength in oxides is only 20 kcal for Na and 32 kcal for Ca, which is much lower than the bond strength of 106 kcal for Si in its oxides [5]. Once is separated from the glass network, the Na and Ca ions are exposed to a repulsive electrostatic interaction produced by Auger and secondary electrons in the irradiation region. The migration process of Na and Ca ions moving away from the irradiated area to the surrounding region has been well observed in our experiments. Figure 4(a) and 4(b) are EDS data taken from the same area of the specimen. EDS data of Figure 4(b) was

taken 10 seconds after Figure 4(a) had been recorded (accumulated dose of $1.2 \times 10^{-13} \text{ C/nm}^2$). The intensity ratio of the Na peak to the Si peak in Figure 4(b) is reduced by 40% compared to that in Figure 4(a). But the ratio of Ca to Si is only reduced by a few percent in Figure 4(b). These EDS data show that the concentration of Na and Ca in the specimen was decreased by the electron beam irradiation. The variation in the positive ion concentration in the specimen certainly changes the inner potential distribution and results in the change in contrast of Fresnel images of the specimen. Thus, in order to correctly interpret the Fresnel contrast images of soda-lime-silica glass, it is necessary to know the amount of electron dosage to the specimen during the experiment.

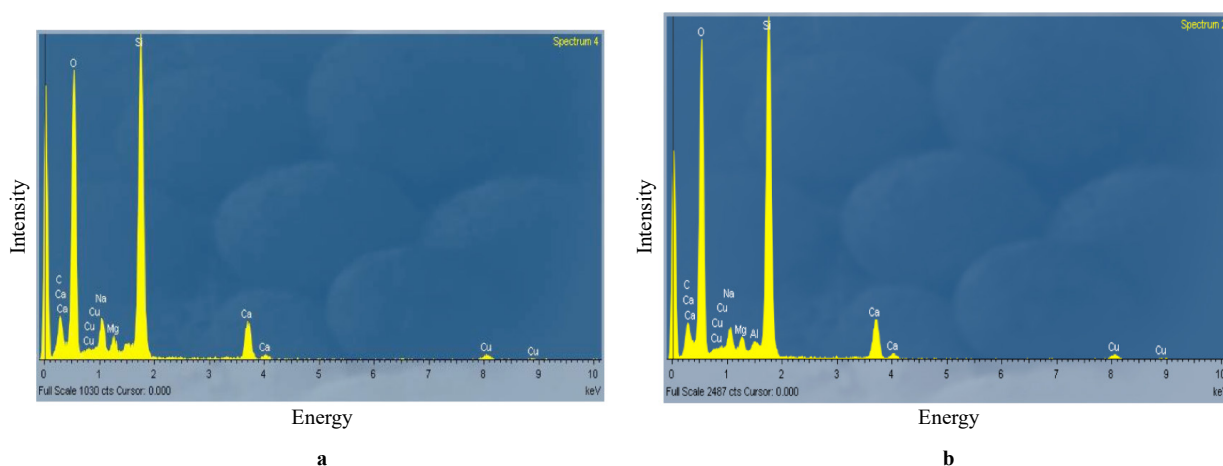


Figure 4. EDS data of soda-lime-silica glass. (a) was recorded with accumulated dose of the electron dose received by the specimen in the observed area was approximately $4 \times 10^{-14} \text{ C/nm}^2$. (b) was taken 10 seconds after Figure 4(a) was recorded. The electron dose received by the specimen in the observed area was approximately $1.2 \times 10^{-13} \text{ C/nm}^2$. The intensity ratio between the Na peak and the Si peak in Figure 4(b) is reduced by 40% compared with that in Figure 4(a).

It was found that at the very beginning of the observation with a beam intensity of $\sim 8 \times 10^{-15} \text{ A/nm}^2$ the specimen did not show any contrast, regardless of the objective lens focus value. However, a few seconds later when the electron dose received by the specimen in the observed area was approximately $4 \times 10^{-14} \text{ C/nm}^2$, Fresnel contrast appeared and its intensity increased with the observation time. After about 10 seconds of electron beam exposure, Figure 5(a) and 5(b) were taken with the objective lens underfocus and overfocus by about $3 \mu\text{m}$, respectively. These images clearly show interpenetrated phase separation in the soda lime silica glass. The cross-section of the interpenetrating structure in Figure 5 is estimated to be 6 nm. As the electron dose received by the specimen increased, the contrast between the two regions increases without significantly altering the length-scale of the phase structures. During the observation process, the position and the size of the electron beam were kept unchanged before taking the images. Images taken from various locations of the specimen were all similar to that shown in Figure 5. However, the irradiation time of the specimen required for the appearance of Fresnel contrast in the thicker area was longer than that in the thinner areas.

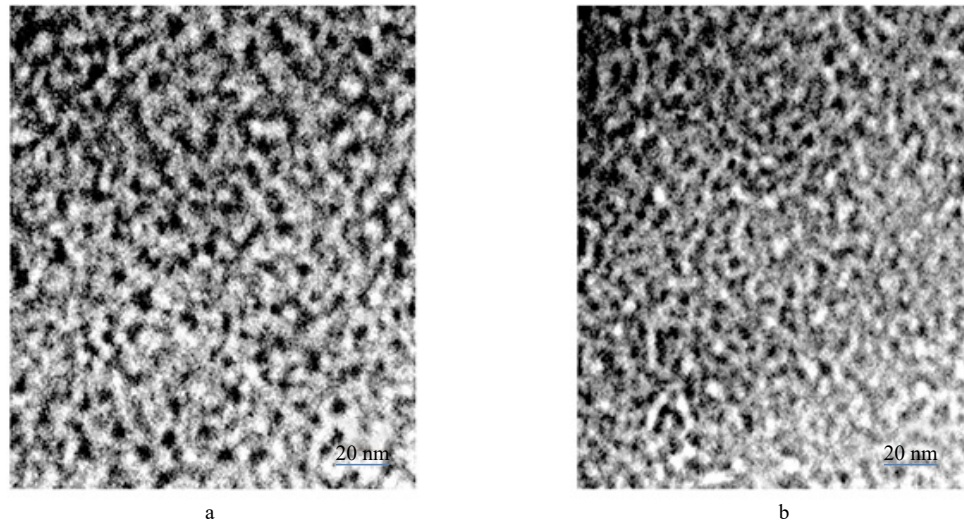


Figure 5. Images of soda-lime-silica glass specimens, taken with the objective lens (a) underfocus and (b) overfocus by about 3 μm , respectively. The images clearly show interpenetrated phase separation in the soda-lime-silica glass. The cross-section of the interpenetrating structure in Figure 5 is estimated to be 6 nm.

The fact that images showed no contrast in the initial observation indicates that the inner potential in the soda-lime-silica glass is uniform throughout the specimen before the specimen is exposed to the electron beam. During the irradiation some Na and Ca ions move out from the irradiated area, and the inner potential is reduced more in the regions originally rich in Na and Ca than in the regions originally deficient in Na and Ca. If the concentration of Na and Ca in the un-irradiated specimen is the same everywhere, then the change of the inner potential in all irradiated areas would be uniform after the migration of Na and Ca ions. The Fresnel contrast images of Figure 5 confirm that the distribution of Na and Ca in the soda-lime-silica glass is not uniform. Thus, the contrast between the Na and Ca rich and poor regions can be distinguished in Fresnel contrast images.

During the image acquisition, some Na and Ca ions migrated out from the glass network in the observation area, but the silicon oxide glass network did not change. This is evidenced by the energy loss near edge structure (ELNES) of the Si $L_{2,3}$ -edges, shown in Figure 6. The spectrum in Figure 6 is characterized by the absorption peaks at 106 eV and 108 eV, labeled b and c, and a feature at 105 eV, labeled a. These features are the same as those of Si $L_{2,3}$ -edges obtained from pure silica [20]. If the bonding between Si and O is broken by the irradiation effects, there should be additional absorption in the energy range from 100 eV to 104 eV in the spectrum generated by the intermediate oxidation state of Si [21]. From previous experiments, when the 200 kV electron dose is about $2.7 \times 10^{-12} \text{ C/nm}^2$, which is about 2 orders higher than that used for taking the images in Figure 5, the intensity of Si $L_{2,3}$ -edges of silica specimen in the energy range from 100 eV to 104 eV increased significantly. This indicated that a certain amount of bonds between Si and O in the specimen were broken [22]. When the images of Figure 5 were taken, the electron dose on the specimen was approximately $8 \times 10^{-14} \text{ C/nm}^2$, and no changes in the ELNES of Si $L_{2,3}$ -edges were observed. It is thus concluded that under the experimental conditions used to acquire the images of Figure 5, some Na and Ca ions migrated out from the irradiated area, but the silicon oxide glass network was basically unchanged. Therefore, the interconnected nano structure revealed by the Fresnel contrast images shown in Figure 5 is the original phase-separated structure of the glass.

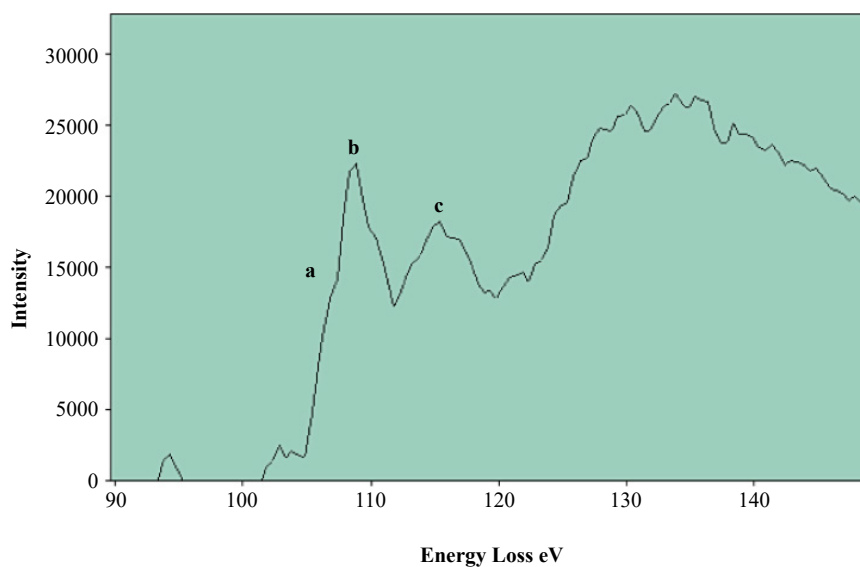


Figure 6. The Si $L_{2,3}$ -edges in EELS recorded from soda-lime-silica glass. It is characterized by the absorption peaks at 106 eV and 108 eV, labeled b and c, with a feature at 105 eV, labeled a. These features are the same as those of Si $L_{2,3}$ -edges obtained from pure silica.

4. Conclusions and discussions

Based on the fundamental principle of materials science that physical properties of materials must correlate with their internal structures, it is essential to understand the phase-separated structure at the nanoscale for various glasses. TEM is a technique often-chosen to study the nanostructure of materials due to its high spatial resolution. However, two significant obstacles exist that prevent its wide use in glass research. One is that the main glass composition contains light elements. They distribute in various regions and produce only little diffraction contrast in TEM images. Such low-contrast images make it hard to recognize the types and sizes of the phases. The second problem is that due to the radiation effect of the high-energy electron beams, the structures of glasses are easily altered under TEM observation. Simply claiming TEM image results as the glass structures without accounting for the radiation effects on the specimens could be erroneous and must be avoided. Although using a traditional carbon replica is one way to mitigate these two problems, the spatial resolution is often insufficient in the study.

Our experimental results show that the Fresnel contrast technique can overcome the difficulties of using TEM in the study of glass structures. The technique might be a practically useful way to characterize glass nanophase structures. Also, the Fresnel contrast technique is more convenient and reliable than the ion exchanging technique. In addition, it does not introduce foreign elements into the specimen. Thus, the same specimen could be used for subsequent chemical and structural analysis by analytical TEM techniques, such as EDS and EELS [14,23]. More applications of the Fresnel contrast technique to the study of glass system structures are expected.

Acknowledgments

The authors acknowledge support of the National Center for Electron Microscopy, Lawrence Berkeley Lab, which is supported by the U.S. Department of Energy under Contract # DE-AC02-05CH11231.

Conflict of interest

There is no conflict of interest for this study.

References

- [1] Vogel, W. *Chemistry of Glass*; The American Ceramic Society: Ohio, OH, USA, 1985.
- [2] Pye, L.; Ploetz, L.; Manfredo, L. Physical properties of phase separated soda-silica glasses. *J. Non-Crystalline Solids* 1974, *14*, 310–321, [https://doi.org/10.1016/0022-3093\(74\)90041-6](https://doi.org/10.1016/0022-3093(74)90041-6).
- [3] Porai-Koshits, E.; Averjanov, V. Primary and secondary phase separation of sodium silicate glasses. *J. Non-Crystalline Solids* 1968, *1*, 29–38, [https://doi.org/10.1016/0022-3093\(68\)90004-5](https://doi.org/10.1016/0022-3093(68)90004-5).
- [4] Mazurin, O.V.; Porai-Koshits, E.A. *Phase separation in Glass*; North-Holland: Amsterdam, Netherlands, 1984.
- [5] Varshneya, A.K.; Mauro, J.C. *Fundamentals of Inorganic Glasses*; Elsevier: Amsterdam, Netherlands, 2019.
- [6] Doremus, R.H.; Turkalo, A.M. Phase Separation in Pyrex Glass. *Science* 1969, *164*, 418.
- [7] Doremus, R.H. Ion exchange with a two-phase glass. *J. Phys. Chem.* 1968, *72*, 2665–2666, <https://doi.org/10.1021/j100853a076>.
- [8] Graham, M.B.W.; Shuldiner, A.T. *Corning and the Craft of Innovation*; Oxford University Press: Oxford, UK, 2001; pp. 54–58.
- [9] Cormier, L.; Calas, G.; Beuneu, B. Structural changes between soda-lime silicate glass and melt. *J. Non-Crystalline Solids* 2010, *357*, 926–931, <https://doi.org/10.1016/j.jnoncrysol.2010.10.014>.
- [10] Greaves, G.N.; Fontaine, A.; Lagarde, P.; Raoux, D.; Gurman, S.J. Local structure of silicate glasses. *Nature* 1981, *293*, 611–616, <https://doi.org/10.1038/293611a0>.
- [11] Gaskell, P.H.; Eckersley, M.C.; Barnes, A.C.; Chieux, P. Medium-range order in the cation distribution of a calcium silicate glass. *Nature* 1991, *350*, 675–677, <https://doi.org/10.1038/350675a0>.
- [12] Cheng, S.; Laboratory, L.B.N.; Song, C.; Ercius, P.; Shangcong, C.; Peter, E. Nanophase structures of commercial Pyrex glass cookware made from borosilicate and from soda lime silicate. *Phys. Chem. Glas. Eur. J. Glas. Sci. Technol. Part B* 2015, *56*, 108–114, <https://doi.org/10.13036/17533562.56.3.108>.
- [13] Cheng, S.; Song, C.; Ercius, P.; Cionea, C.; Hosemann, P. Indentation cracking behavior and structures of nanophase separation of glasses. *Phys. Chem. Glasses Eur. J. Glass Sci. Technol. B* 2017, *58*, 237–242.
- [14] Williams, D.B.; Carter, C.B. *Transmission Electron Microscopy*; Springer: New York, NY, USA, 2009; pp. 163–400, e-ISBN 978-0-387-76501-3.
- [15] Ruhle, M.; Wilkens, M. Defocusing contrast of cavities 1. Theory. *Crystal Lattice Defects.* 1975, *6*, 129–140
- [16] Stobbs, W.M. Electron Microscopical Techniques for The Observation of Cavities. *J. Microsc.* 1979, *116*, 3–13, <https://doi.org/10.1111/j.1365-2818.1979.tb00184.x>.
- [17] Pantano, C.G.; Madey, T.E. Electron beam damage in Auger electron spectroscopy. *Appl. Surf. Sci.* 1981, *7*, 115.
- [18] Jiang, N.; Silcox, J. Electron irradiation induced phase decomposition in alkaline earth multi-component Oxide Glass. *J. Appl. Physics.* 2002, *92*, 2310–2316.
- [19] Cheng, S.; Logunov, S.; Streltsov, A. Laser-Induced Swelling of Borosilicate Glasses-An Analysis of Associated Microstructural Development. *Int. J. Appl. Glas. Sci.* 2014, *5*, 267–275, <https://doi.org/10.1111/ijag.12067>.
- [20] Garvie, L.; Buseck, P.R. Bonding in Silicates: Investigation of the Si L_{2,3} edge by Parallel Electron Energy—Loss Spectroscopy. *Am. Mineral.* 1999, *84*, 946–964.
- [21] Dori, L.; Bruley, J.; DiMaria, D.J.; Batson, P.E.; Tornello, J.; Arienzo, M. Thin-oxide Dual-electron-injector Annealing Studies Using Conductivity and Electron Energy Loss Spectroscopy. *J. Appl. Phys.* 1991, *69*, 2317.
- [22] Cheng, S.; Schiefelbein, S.L. The Impact of Disorder on the Urbach Absorption Edge of Silica Measured by Electron Energy Loss Spectroscopy. *In Proceeding of ACerS Glass & Optical Materials Division Spring Meeting*; Wiley & Sons: New York, NY, USA, 2007.
- [23] Egerton, R.F. *Electron Energy-Loss Spectroscopy in Electron Microscopy*; Springer Science & Business Media: New York, NY, USA, 2011.